An Extended Kalman Filter for Nonsmooth Attitude Control Design of Quadrotors using Quaternion Representation

Adha Cahyadi[1], Andreas P. Sandiwan[1], Samiadji Herdjunanto[1]
[1,3]Department of Electrical and Information Engineering, Universitas Gadjah Mada, Indonesia

Article Info

Article historys:

Received Nov 24, 2021
Revised May 24, 2022
Accepted Jun 11, 2022

Keywords:

Sliding mode control
Attitude control
Extended kalman filter
Quaternion representation

ABSTRACT

This paper proposed Extended Kalman Filter specifically designed for nonlinear and nonsmooth control system applied in Autonomous Quadrotor Control such as sliding mode control. Many controllers focused on global stability usually consider exact parameters through measurements. Such assumptions are not always possible due to the unavailability of sensors or unmeasurable state in real-life condition. In this paper, we consider only the angular velocity is possible for measurement, i.e., only gyroscope measurement is available. This condition is known as omega-state-measurement (OSM). Without loss of generality, for theoretical simplification beside gyroscope measurement, we assume the orientation measurement represented in quaternion is also available. Additive random gaussian noise is included to the measurement model to be used in Kalman Filter. Finally the proposed Extended Kalman Filter implemented in a PD Sliding Mode controller is simulated using many scenarios to verify its effectiveness. The Kalman Filter works well in spite of model error and disturbance.

Corresponding Author:

Adha Cahyadi,
Department of Electrical and Information Engineering,
Universitas Gadjah Mada,
Jl. Grafika No. 2, Depok, Sleman, Yogyakarta, Indonesia.
Email: adha.cahyadi@ugm.ac.id

1. INTRODUCTION

Attitude control is the process of controlling the orientation of a rigid body with respect to an inertial reference frame. The rigid bodies of interest are, for example, aircraft, helicopter, satellites, and robot arm. This problem has been an object of extensive research for decades.

The first thing that can come into concern is the way the attitude or orientation is represented. There are three approaches to represent the attitude of a rigid body, i.e. Euler angles, rotation matrix, and quaternion [1]. Euler angle representation is popular because of it provides minimal representation of rotation with its 3 elements. However, its weakness lies in the existence of singularities at several values of Euler angles [2]. Rotation matrix can represent rotation uniquely, but using rotation matrix usually requires complicated mathematics. Such inherent property means that control law based on rotation matrix is difficult to design. Rotation matrix also presents additional problem because it has 9 elements, which do not constitute minimal attitude representation. Quaternion representation can be used to circumvent the drawbacks of the two preceding representations. A quaternion's 4 elements provide global minimal nonsingular representation [3]. Despite its advantage, quaternion is not without drawback. Quaternions double-cover the space of rotation, so one orientation has two corresponding antipodal quaternions. In several cases, if the control law is not designed carefully, the rigid body may have to go through a unnecessary large-angle rotation path instead of a small-angle one, which is called unwinding. However, this unwinding phenomenon can be avoided by careful design process like the one presented in [4].

The first challenge in designing quaternion-based attitude control law is the nonlinear differential equations for dynamics and kinematics. There are many control methods that can be used in solving nonlinear control problem, such as linearization-based methods, integral control, feedback linearization, backstepping, and sliding mode control [5]. One of the effective methods is sliding mode control, which uses sliding variables. Sliding variables can simplify Lyapunov analysis by forming a hierarchy of simple reduced order systems [6]. In addition, it can be made robust against external disturbances and unknown dynamics [5].

For years, researchers have employed sliding mode control in designing quaternion-based attitude control law. In 1995, Lo and Chen proposed smoothing model-reference sliding mode control (SMRSMC) algorithm for spacecraft attitude tracking control [7]. The developed control law can successfully track time-varying attitude set point and improves the undesirable transient response induced in conventional sliding-mode controller. Jan and Chiou in [8] developed a robust tracking control scheme using sliding mode control for spacecraft large angle maneuver within minimum time. Their published paper showed satisfactory result for constant set point. Unfortunately, the performance of their controller under changing set point was not evaluated. Yeh in [9] developed sliding mode attitude tracking controller and sliding-mode adaptive attitude tracking controller for spacecraft with thrusters. It was shown that the developed controllers were able to track changing set points and perform well under inertia matrix uncertainty as well as disturbance. Guo, Song, and Li in [10] presented two terminal sliding mode controllers that could achieve finite-time stability. In addition, it could avoid unwinding phenomenon is robust against bounded disturbance. Unfortunately, the developed control laws were complicated. Tiwari, Janardhanan, and Nabi in [11] presented a robust adaptive finite-time sliding mode attitude tracking control for rigid spacecraft. The simulation of their control law demonstrated the effectiveness of the developed control law under the presence of external disturbance, inertia uncertainties, and constrained control input. Despite its effectiveness, the control law was also complicated. Meanwhile, the weakness of [7] and [9] was their inability to avoid unwinding, as demonstrated by Lopez and Slotine in [4]. To address the weaknesses of previous studies, Lopez and Slotine in [4] developed 3 control laws based on sliding mode scheme. One of them, namely nonlinear PD sliding control, is interesting to be studied further because it is able to avoid unwinding phenomenon, perform well under bounded disturbance, and much simpler than the control laws in [10] and [11].

In a realistic scenario, the quantities measured by sensors are always disturbed by random noise. Thus, it is reasonable to include a state estimator that is able to filter random noise into a control algorithm. Roughly speaking, existing state estimation studies can be divided into two groups. In the first group, the state estimation is the primary concern; although a particular study incorporates a control algorithm, the result of state estimation is not used by the control algorithm. In the second group, the state estimation result is used by the control algorithm. The second group represents the realistic scenario because the control algorithm must use result from state variable estimation, which filters out random noise that disturbs true state variable values during measurement process by sensors. The family of filtering algorithm that is very popular is the Kalman filter family, which includes Kalman Filter (for linear systems), and Extended Kalman Filter (EKF) as well as Unscented Kalman Filter (UKF) (for nonlinear systems). There are several studies in the automatic control field that present a coupled estimator-controller using Kalman filter family. Jafarboland, Sadati, and Momeni in [12] presented a robust tracking control scheme of a satellite for large rotational maneuvers. The estimator featured combined discrete and continuous EKF, while the controller employs sliding mode method with perturbation estimation. The estimator was proven to be capable of achieving small estimation error, while the controller was able to drive the state variable values close to the desired set points. Tarhan and Altug in [13] presented a coupled estimator-controller scheme with catadioptric camera. The attitude of the quadrotor is estimated using EKF, and the result of attitude estimation is incorporated into control law calculation. The experimental results showed that the coupled estimator-controller can yield bounded attitude error that is close to the set points. Kwon, Lee, and You in [14] presented a sliding mode attitude control for quadrotor that incorporated EKF for state estimation. Stability near the desired set points can be reached, but unfortunately, the study lacks the explanation for the stability of the control algorithm that is coupled with EKF. All of [12], [13], and [14] used Euler angle attitude representation, not quaternion.

The main interest of this paper is the nonlinear PD sliding control algorithm in [4]. The reason why it is interesting is that it is simple and is capable of performing attitude tracking task under bounded disturbance, which has been demonstrated in the paper. However, the algorithm has not incorporated any state estimation method. Other previous studies of sliding mode attitude control already reviewed here have not incorporated any state estimation method as well. Thus, it is of interest to develop a sliding mode controller coupled with EKF estimator. The main contribution of this work is the improvement of nonlinear PD sliding controller from [4] by attaching a state estimator using EKF. The main reason for using EKF is that it has been the workhorse of attitude determination for satellites [15], so it can be expected that EKF will work well for the problem presented in this paper. In addition, it also provides an ready-to-use algorithm for filtering noise from measurement.

The remainder of this paper is arranged as follows. First, Section 2 explains the plant dynamics. Next, Section 3 explains the design of the control law that is used to achieve control objective. Section 4 explains the design and the numerical simulation result of the attitude estimator. Section 5 proceeds by coupling the estimator and the controller. The main result of this research is shown in Section 5. Section 6 ends this paper by a conclusion.

2. PLANT DYNAMICS

The plant is a rotating rigid body whose dynamics is described using quaternion representation. Quaternion is a standard representation that can be found in many textbooks in flight dynamics such as in [16]. A quaternion describes rotation in 3 dimensions similarly to a complex number describes rotation in 2 dimensions. It provides global nonsingular parameterization of the space of rotation at the cost of using 4 real numbers instead of 3 (like Euler angles) and double-covering the space of rotation. A quaternion **q** consists of scalar part q_0 and vector part **q** that has 3 components, i.e.

$$\boldsymbol{q} = \begin{bmatrix} q_0 \\ \vec{q} \end{bmatrix} \tag{1}$$

where $q_0 \in \Re$ and $\vec{q} \in \Re^3$.

The inverse of a quaternion **q** is the conjugate quaternion $\boldsymbol{q}* = \begin{bmatrix} q_0 \\ -\vec{q} \end{bmatrix}$. Quaternions for representing rotation are constrained to have unit nowm, i.e. $\|\mathbf{q}\| = 1$; this kind of quaternion is called unit quaternion. The product between two quaternions, denoted by multiplication operator ⊗, is defined as

$$\boldsymbol{p} \otimes \boldsymbol{q} = \begin{bmatrix} p_0 q_0 - \vec{p}^T \vec{q} \\ p_0 \vec{q} + q_0 \vec{p} + \vec{p} \times \vec{q} \end{bmatrix}. \tag{2}$$

The quaternion attitude dynamics is written as

$$\dot{\mathbf{q}} = \frac{1}{2} \mathbf{q} \otimes \begin{bmatrix} 0 \\ \boldsymbol{\omega} \end{bmatrix}, \qquad \mathbf{J}\dot{\boldsymbol{\omega}} = -\boldsymbol{\omega} \times \mathbf{J}\boldsymbol{\omega} + \boldsymbol{\tau}. \tag{3}$$

where $\boldsymbol{\omega} \in \Re^3$ is the angular velocity with respect to body frame, **J** is a symmetric 3-by-3 inertia matrix, and $\boldsymbol{\tau} \in \Re^3$ is the control input torque.

3. CONTROL LAW DESIGN

The control law design in this paper is based on [4]. However, in this paper, the external disturbance and unknown dynamics are not considered. First, the error quaternion $\mathbf{q}_e$ is defined as $\boldsymbol{q}_e \equiv \boldsymbol{q}_d * \otimes \boldsymbol{q}$ where $\mathbf{q}_d*$ is the conjugate of the desired quaternion and **q** is the current quaternion at time t, $\mathbf{q} = \mathbf{q}(t)$ (the explicit time dependence is omitted for the sake of brevity). Meanwhile, the angular velocity error is defined as $\boldsymbol{\omega}_e \equiv \boldsymbol{\omega} - \boldsymbol{\omega}_d$, where $\boldsymbol{\omega}_d$ is the desired angular velocity. The dynamics of the error quaternion is

$$\dot{\boldsymbol{q}}_e = \tfrac{1}{2} \boldsymbol{q}_e \otimes \begin{bmatrix} 0 \\ \boldsymbol{\omega} \end{bmatrix}. \tag{4}$$

The design of the control law begins with the sliding variable **s**, which is defined as

$$\boldsymbol{s} \equiv \boldsymbol{\omega}_e + \lambda\, sgn_+(q_{e0})\, \vec{q}_e, \tag{5}$$

with $\lambda > 0$ and

$$sgn_+ \equiv \begin{cases} 1, x \geq 0 \\ -1, x < 0 \end{cases} \tag{6}$$

Let the manifold S be defined as $S \equiv \{(\vec{q}_e, \boldsymbol{\omega}_e) : \boldsymbol{s}(\vec{q}_e, \boldsymbol{\omega}_e) = \mathbf{0}\}$. It has been shown in [4] that, if the manifold S is made invariant via feedback, the error quaternion $\mathbf{q}_e$ converges to identity quaternion exponentially.

The nonlinear PD sliding control law proposed in [4] is

$$\boldsymbol{\tau} = \boldsymbol{J}\dot{\boldsymbol{\omega}}_d + \boldsymbol{\omega} \times \boldsymbol{J}\boldsymbol{\omega} - \lambda \boldsymbol{J}\, sgn_+(q_{e0}) \frac{d\vec{q}_e}{dt} - \boldsymbol{K}_{att}\boldsymbol{s}, \tag{7}$$

Where $\mathbf{K}_{att}$ is a diagonal, positive definite 3-by-3 matrix. Without disbance and unknown dynamics, this controller yields asymptotic stability. As in [4], we take the Lyapunov function as

$$V = \boldsymbol{s}^T \boldsymbol{J} \boldsymbol{s}. \tag{8}$$

Differentiation with respect to time yields

$$\begin{aligned} \dot{V} &= 2\mathbf{s}^T \mathbf{J}\dot{\mathbf{s}} \\ &= 2\mathbf{s}^T \left(\mathbf{J}\dot{\boldsymbol{\omega}} - \mathbf{J}\dot{\boldsymbol{\omega}}_d + \lambda \mathbf{J}\, \mathrm{sgn}_+(q_{e0}) \dot{\vec{q}}_e \right) \\ &= 2\mathbf{s}^T \left(-\boldsymbol{\omega} \times \mathbf{J}\boldsymbol{\omega} + \boldsymbol{\tau} - \mathbf{J}\dot{\boldsymbol{\omega}}_d + \lambda \mathbf{J}\, \mathrm{sgn}_+(q_{e0}) \dot{\vec{q}}_e \right). \end{aligned} \tag{9}$$

Substituting equation (7) into (9) yields

$$\dot{V} = -2\boldsymbol{s}^T\boldsymbol{K}_{att}\boldsymbol{s} = -2\sum_{i=1}^{3} k_i s_i^2, \quad (10)$$

which mathematically proves asymptotic stability.

The preceding mathematical analysis is supported with numerical simulation result. For this purpose, the set point is given via yaw (ψ), pitch (θ), and roll (φ) (YPR) angle. The desired YPR values are time-varying, given by $\psi_d(t) = \theta_d(t) = \varphi_d(t) = (\pi/6)\cos(0.5t)$. These YPR values are then converted to yield $q_d(t)$. Figure 1 shows the attitude tracking result in quaternion representation. It can be seen that the output curve (blue) oervlaps with desired curve (red) after several seconds.

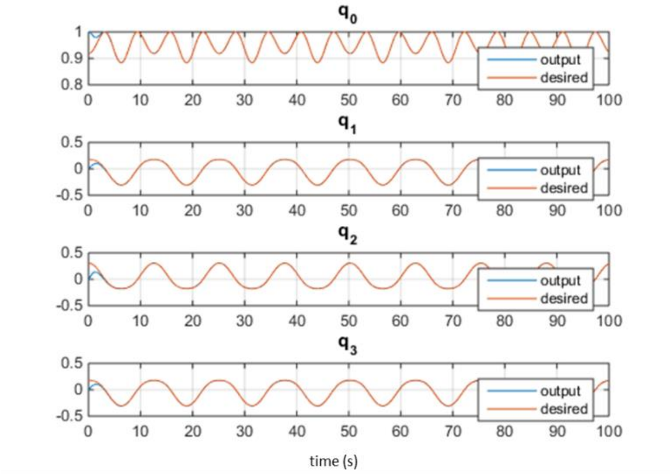

Figure 1. Attitude tracking in quaternion representation.

4. ATTITUDE ESTIMATOR

Before coupling the attitude estimator with the controller, it is important to know the estimator's performance when it is decoupled from the controller. In other words, we will evaluate the performance of the estimator alone, and the control law is calculated using exact state variable values, not the estimated ones. After establishing the good attitude estimator in this section, that estimator will be coupled with the contro law in the next section. This section is divided into two subsections. The first subsection explains the derivation of the estimator algorithm, while the second subsection evaluates the performance of the estimator.

4.1. Derivation of Estimator Algorithm

The attitude estimator used in this paper is the Extended Kalman Filter (EKF). EKF is an extension of continuous-time Kalman Filter for nonlinear system. The nonlinear dynamic model and nonlinear measurement model are respectively expressed as

$$\dot{\boldsymbol{x}} = \boldsymbol{f}(\boldsymbol{x}, t) + \boldsymbol{G}\boldsymbol{w}, \quad \mathbf{w} \sim N\big(0, Q(t)\big) \quad (11)$$

and

$$\boldsymbol{z} = \boldsymbol{h}(\boldsymbol{x}, t) + \boldsymbol{v}, \quad \mathbf{v} \sim N\big(0, R(t)\big) \quad (12)$$

where **w** and **v** are process and measurement noise, respectively. Following the Kalman Filter relation, **w** and **v** are assumed to be zero-mean random variables that are uncorrelated w.r.t. time where the covariance are Q(t) and R(t), respectively. The explicit time dependence for **x**, **G**, **z**, **w**, and **v** have been omitted for the sake of brevity. In our case, the process noise is assumed to be absent. The state variable is $\boldsymbol{x} = \begin{bmatrix}\boldsymbol{q} \\ \boldsymbol{\omega}\end{bmatrix}$, so there are 7 elements in the vector **x**. The state dynamics **f(x,** *t*) is the closed-loop dynamics of the system, provided by equation (3) together with control law (7).

There are two options for the state measurement function **h**(**x**, *t*). The first option is

$$\boldsymbol{h}(\boldsymbol{x}, t) = \begin{bmatrix}\boldsymbol{0}_{4\times4} & \boldsymbol{0}_{4\times3} \\ \boldsymbol{0}_{3\times3} & \boldsymbol{I}_{3\times3}\end{bmatrix}\begin{bmatrix}\boldsymbol{q} \\ \boldsymbol{\omega}\end{bmatrix} \triangleq \boldsymbol{H}_{OSM}\begin{bmatrix}\boldsymbol{q} \\ \boldsymbol{\omega}\end{bmatrix}, \quad (13)$$

where $\boldsymbol{0}_{m\times n}$ denotes an *m*-by-*n* zero matrix and $\boldsymbol{I}_{m\times m}$ denotes an *m*-by-*m* identity matrix. The first option implies that only the angular velocity is available for measurement. This represents the situation where only gyroscope measurement is available. This option will be called omega-state-measurement (OSM). The second option is

$$\boldsymbol{h}(\boldsymbol{x}, t) = \boldsymbol{I}_{7\times7}\begin{bmatrix}\boldsymbol{q} \\ \boldsymbol{\omega}\end{bmatrix} \triangleq \boldsymbol{H}_{FSM}\begin{bmatrix}\boldsymbol{q} \\ \boldsymbol{\omega}\end{bmatrix}, \quad (14)$$

which means that all state variable is observable. This option represents the theoretical simplification of the situation where, in addition to gyroscope measurement, orientation measurement represented in quaternion is also available. In the real world, orientation can be measured using, for example, accelerometer and magnetometer. This option will be called full-state-measurement (FSM). In this option, the measurement of **q** is directly disturbed by additive random gaussian noise. Using the available measurement matrix, the predicted state measurements are

$$\hat{\boldsymbol{z}} = \boldsymbol{H}_{OSM}\hat{\boldsymbol{x}} \quad (15)$$

for the OSM option, and

$$\hat{\boldsymbol{z}} = \boldsymbol{H}_{FSM}\hat{\boldsymbol{x}} \quad (16)$$

for the FSM option. The differential equation for the covariance matrix **P** is

$$\dot{\boldsymbol{P}} = \boldsymbol{FP} + \boldsymbol{PF}^T + \boldsymbol{GQG}^T - \bar{\boldsymbol{K}}\boldsymbol{R}\bar{\boldsymbol{K}}^T \quad (17)$$

where F is the linearization of $\boldsymbol{f}(\boldsymbol{x}, t)$ near to $\hat{\boldsymbol{x}}$.
Using where H is the linearization of $\boldsymbol{h}(\boldsymbol{x}, t)$ near to $\hat{\boldsymbol{x}}$, the Kalman gain matrix $\bar{\boldsymbol{K}}$ is calculated as

$$\bar{\boldsymbol{K}} = \boldsymbol{PHR}^{-1}. \quad (18)$$

The Kalman gain matrix $\bar{\boldsymbol{K}}$ is divided into two parts, whose purpose is going to be clear soon. The first part $\bar{\boldsymbol{K}}_1$ consists of the 1st to 4th row of $\bar{\boldsymbol{K}}$, while the second part $\bar{\boldsymbol{K}}_2$ consists of the 5th to 7th row of $\bar{\boldsymbol{K}}$. Both $\bar{\boldsymbol{K}}_1$ and $\bar{\boldsymbol{K}}_2$ have 7 columns like $\bar{\boldsymbol{K}}$ does.

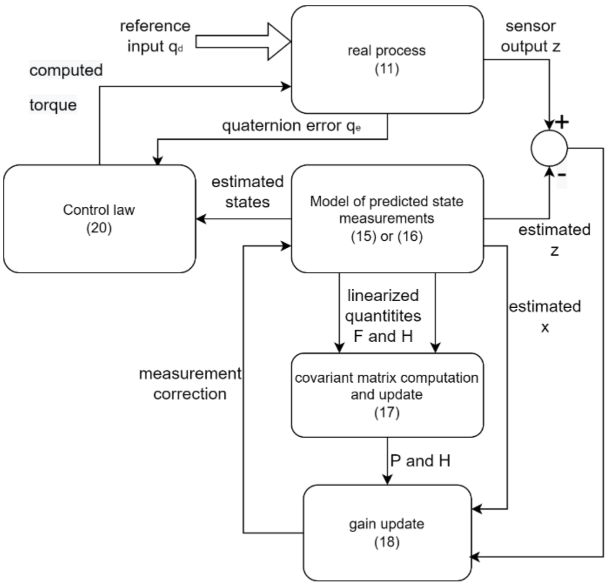

Figure 2. Complete block diagram of proposed control system

The differential equation for the state estimate of the closed-loop system is divided into three parts. The first part is calculating the estimate for quaternion, i.e.

$$\dot{\hat{\boldsymbol{q}}} = \frac{1}{2}\hat{\boldsymbol{q}} \otimes \begin{bmatrix} 0 \\ \hat{\boldsymbol{\omega}} \end{bmatrix} + \bar{\boldsymbol{K}}_1(\boldsymbol{z} - \hat{\boldsymbol{z}}). \quad (19)$$

The second part is calculating the control law $\boldsymbol{\tau}$. The control law calculation is using estimated $\hat{\boldsymbol{\omega}}$, i.e.

$$\boldsymbol{\tau} = \boldsymbol{J}\dot{\boldsymbol{\omega}}_d + \hat{\boldsymbol{\omega}} \times \boldsymbol{J}\hat{\boldsymbol{\omega}} - \lambda\boldsymbol{J}\, sgn_+(q_{e0})\, \dot{\vec{q}}_e - \boldsymbol{K}_{att}\boldsymbol{s} \quad (20)$$

where the estimated value of the angular velocity is solved from

$$\dot{\hat{\boldsymbol{\omega}}} = \boldsymbol{J}^{-1}(-\hat{\boldsymbol{\omega}} \times \boldsymbol{J}\hat{\boldsymbol{\omega}}) + \boldsymbol{J}^{-1}\boldsymbol{\tau} + \bar{\boldsymbol{K}}_2(\boldsymbol{z} - \hat{\boldsymbol{z}}). \quad (21)$$

Finally, the **F** and **H** matrix in equation (17) is approximated by

$$\boldsymbol{F} \approx \left.\frac{\partial \boldsymbol{f}(x,t)}{\partial x}\right|_{x=\hat{x}}, \boldsymbol{H} \approx \left.\frac{\partial \boldsymbol{h}(x,t)}{\partial x}\right|_{x=\hat{x}}. \quad (22)$$

which results in a 7-by-7 square matrix, respectively. The complete system consisting the estimated state and the modified control law (20) is illustrated in Figure 2. It seen that the previously unrealistic control law can be successfully implemented using the proposed scenario.

4.2. Numerical Simulation Result of Attitude Estimator

The attitude estimator that has been derived is then tested in numerical simulation. Numerical simulation is conducted using MATLAB script with ode45 solver. Because the process noise is assumed to be absent, the process noise covariance Q(t) is equal to zero. The measurement noise is generated using randn function that generates random numbers under normal distribution. The standard deviation for measurement noise σ_v is equal to 10^{-3}, while the measurement noise covariance is $R(t) = \sigma_v^2 = 10^{-6}$. The initial value of covariance matrix **P** is $\boldsymbol{P}_0 = 10^{-8}\boldsymbol{I}_{7\times7}$. The set points are the same as the set points in the previous section, i.e. $\psi_d(t) = \theta_d(t) = \varphi_d(t) = \frac{\pi}{6}cos(0.5t)$. The control law is calculated using exact state variable values. The initial values of the estimated quaternion and angular velocity are also disturbed by random noise. Both OSM and FSM cases are simulated and their results are evaluated.

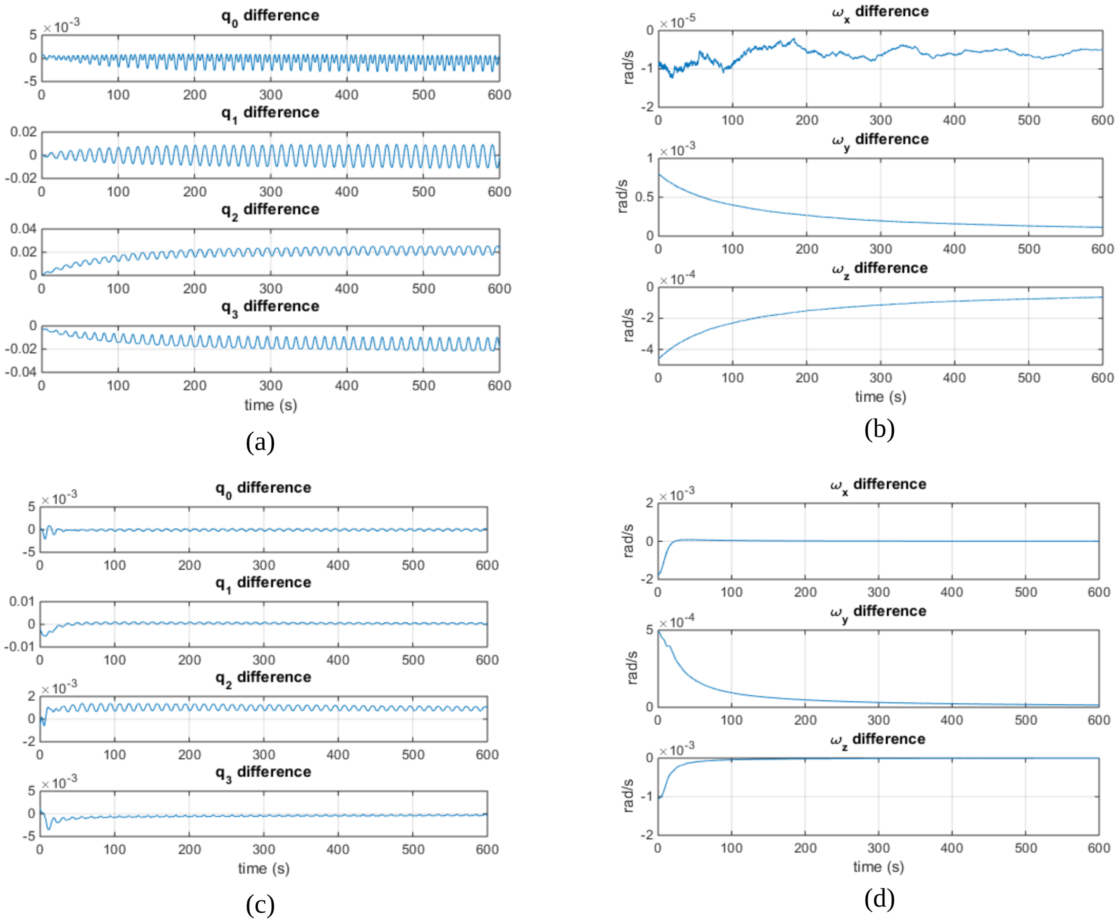

Figure 3. (a) Difference between estimated and exact quaternion, OSM case; (b) Difference between estimated and exact angular velocity, OSM case; (c) Difference between estimated and exact quaternion, FSM case; (d) Difference between estimated and exact angular velocity, FSM case.

First, we evaluate the situation where only the angular velocity $\boldsymbol{\omega}$ is available for measurement, or the OSM case. We do not show the output curve of the quaternion because it is the same as Figure 1. Figure a shows the difference between estimated and exact quaternion and Figure b the difference between estimated and exact angular velocity. It can be seen that although the estimation difference of $\boldsymbol{\omega}$ converges toward zero, the estimation difference of **q** gets larger along with time. These results demonstrates that accurate attitude estimate cannot be achieved if only the angular velocity is available for measurement.

After we have evaluated the situation where only $\boldsymbol{\omega}$ is available for measurement, we now evaluate the situation where both the orientation, represented by **q**, and the angular velocity are available for the measurement. Again, we do not show the output curve of the quaternion because it is the same as Figure 1. Figure c shows the difference between estimated and exact quaternion and Figure c the difference between estimated and exact angular velocity. It can be seen that the estimation differences of $\boldsymbol{\omega}$ and **q** stay very close to zero and do not diverge. These results show that the FSM option is more suitable for the coupling between attitude estimator and the controller, which will be discussed in the next section. In addition, the values of the EKF parameters, which are provided in the first paragraph of this section, will be used in the estimator-controller coupling. Those parameter values have been shown to be suitable for the noise filtering purpose because the results shown by Figure c and Figure d.

5. ESTIMATOR-CONTROLLER COUPLING

This section is the core of this paper. After developing a good estimator in the previous section, we now proceed into coupling the estimator with the controller. This means that the control law is calculated using estimated state variable values. For the EKF algorithm, FSM option is used. Similar to the previous section, this section is divided into two subsections. The first subsection will explain the estimator-controller algorithm, while the second one will discuss the results of the estimator-controller algorithm.

5.1. Estimator-Controller Algorithm

The EKF algorithm is the same as mentioned in the previous section. Also similarly, the differential equation for the state estimate of the closed-loop system is divided into three parts. The first part is calculating the estimate for quaternion, i.e.

$$\dot{\hat{\boldsymbol{q}}} = \frac{1}{2}\hat{\boldsymbol{q}} \otimes \begin{bmatrix} 0 \\ \hat{\boldsymbol{\omega}} \end{bmatrix} + \bar{\boldsymbol{K}}_1(\boldsymbol{z} - \hat{\boldsymbol{z}}) \tag{23}$$

The second part is calculating the control law. Because the control law is calculated using estimated state variable values, i.e. $\hat{\boldsymbol{q}}$ and $\hat{\boldsymbol{\omega}}$, to avoid confusion with the control law calculated using exact $\mathbf{q}$ and $\boldsymbol{\omega}$, it will be denoted as $\boldsymbol{\tau}$`. It is calculated as

$$\boldsymbol{\tau}` = \boldsymbol{J}\dot{\boldsymbol{\omega}}_d + \hat{\boldsymbol{\omega}} \times \boldsymbol{J}\hat{\boldsymbol{\omega}} - \lambda\, sgn_+(\hat{q}_{e0})\, \dot{\vec{\hat{q}}}_e - \boldsymbol{K}_{att}\hat{\boldsymbol{s}} \tag{24}$$

It can be noted that the sliding variable is also altered into $\hat{\boldsymbol{s}}$, i.e.

$$\hat{\boldsymbol{s}} = \hat{\boldsymbol{\omega}}_e + \lambda\, sgn_+(\hat{q}_{e0})\, \dot{\vec{\hat{q}}}_e, \tag{25}$$

where $\boldsymbol{\omega}_e = \hat{\boldsymbol{\omega}} - \hat{\boldsymbol{\omega}}_d$ and $\hat{\boldsymbol{q}}_e = \boldsymbol{q}_d * \otimes\, \hat{\boldsymbol{q}}$. The third part is calculating the estimated value of the angular velocity, i.e.

$$\dot{\hat{\boldsymbol{\omega}}} = \boldsymbol{J}^{-1}(-\hat{\boldsymbol{\omega}} \times \boldsymbol{J}\hat{\boldsymbol{\omega}}) + \boldsymbol{J}^{-1}\boldsymbol{\tau}` + \bar{\boldsymbol{K}}_2(\boldsymbol{z} - \hat{\boldsymbol{z}}). \tag{26}$$

Because we use the FSM option here, the measurement matrix is $\boldsymbol{H}_{FSM} = \boldsymbol{I}_{7\times7}$.

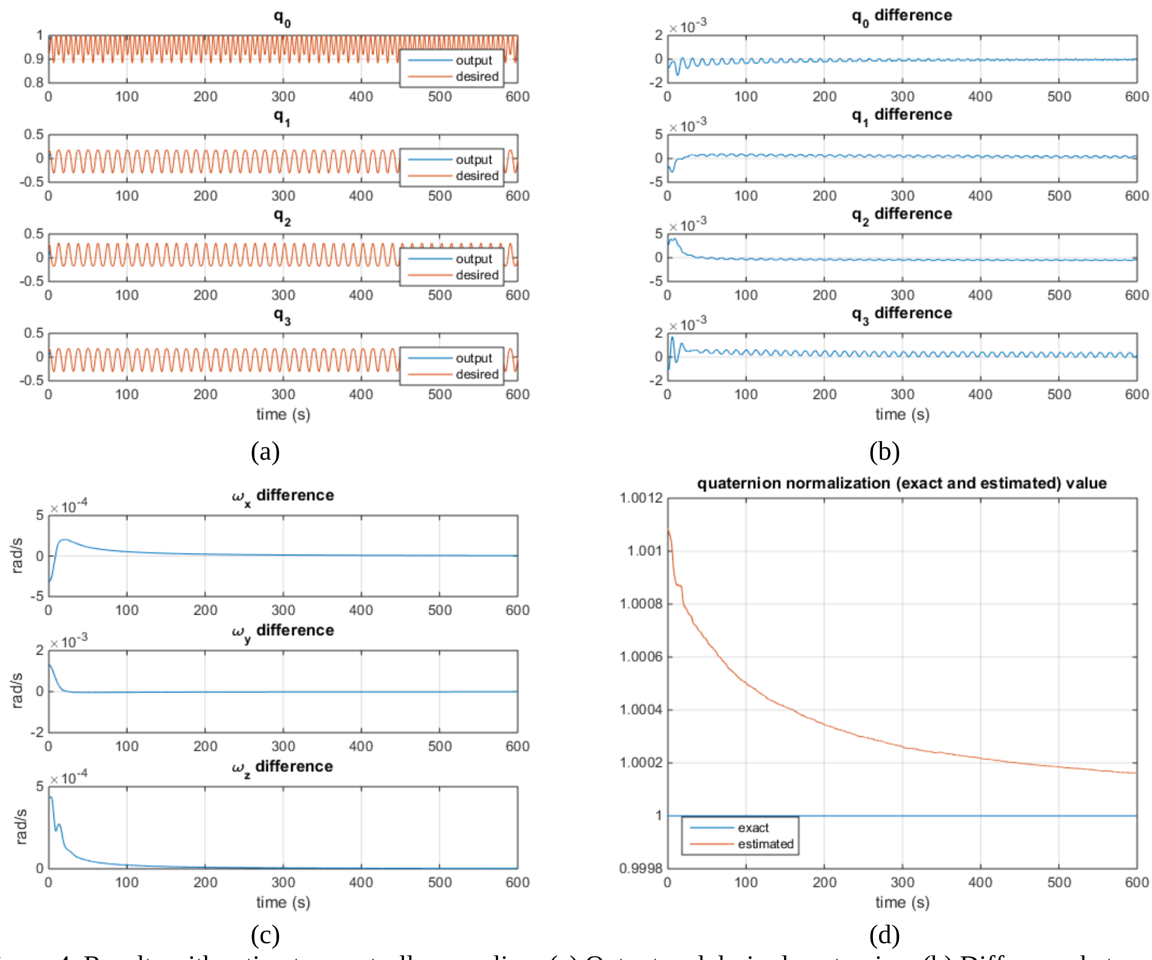

Figure 4. Results with estimator-controller coupling: (a) Output and desired quaternion, (b) Difference between estimated and exact quaternion, (c) Difference between estimated and exact angular velocity, (d) Estimated and exact quaternion norms.

5.2. Evaluation of Estimator-Controller Coupling

The EKF parameters for attitude estimation and simulation settings in MATLAB are the same as in the previous section. The set points are the same, i.e. $\psi_d(t) = \theta_d(t) = \varphi_d(t) = (\pi/6)\,cos(0.5t)$. Figure a shows the output and desired quaternion. It is apparent that the output quaternion can converge to the desired quaternion quickly (the blue curves quickly overlap with the red curves). Next, Figure b shows that the estimated quaternion is close to the exact quaternion. Furthermore, Figure c shows that the estimated angular velocity is also close to the exact angular velocity. The norm of the estimated quaternion is also very close to 1, as shown in Figure d. The good results that occur in the estimator-controller coupling occur because the EKF has been designed properly, as described in the previous section.

6. CONCLUSION

This paper has demonstrated how to design a nonlinear PD sliding controller that is coupled with EKF estimator. The success of the estimator-controller coupling relies on the proper design of the EKF attitude estimator. Simulation results show that the correct design of the EKF attitude estimator will yield good performance when the result of the state estimation is used in calculation of the control law.

REFERENCES

[1] A. P. Sandiwan, A. Cahyadi, and S. Herdjunanto, "Robust proportional-derivative control on SO(3) with disturbance compensation for quadrotor UAV," *Int. J. Control Autom. Syst.*, vol. 15, no. 5, pp. 2329–2342, Oct. 2017, doi: 10.1007/s12555-016-0452-5.

[2] P. I. Corke, *Robotics, vision and control: fundamental algorithms in MATLAB*. Berlin: Springer, 2011.

[3] N. Filipe, M. Kontitsis, and P. Tsiotras, "Extended Kalman Filter for Spacecraft Pose Estimation Using Dual Quaternions," *J. Guid. Control Dyn.*, vol. 38, no. 9, pp. 1625–1641, Sep. 2015, doi: 10.2514/1.G000977.

[4] B. T. Lopez and J.-J. E. Slotine, "Sliding on Manifolds: Geometric Attitude Control with Quaternions," *ArXiv201103648 Cs Eess*, Nov. 2020, Accessed: Jun. 30, 2021. [Online]. Available: http://arxiv.org/abs/2011.03648

[5] H. K. Khalil, *Nonlinear systems*, 3rd ed. Upper Saddle River, N.J: Prentice Hall, 2002.

[6] J.-J. E. Slotine and W. Li, *Applied nonlinear control*. Englewood Cliffs, N.J: Prentice Hall, 1991.

[7] S.-C. Lo and Y.-P. Chen, "Smooth sliding-mode control for spacecraft attitude tracking maneuvers," *J. Guid. Control Dyn.*, vol. 18, no. 6, pp. 1345–1349, Nov. 1995, doi: 10.2514/3.21551.

[8] Y. W. Jan and J. C. Chiou, "Minimum-time spacecraft maneuver using sliding-mode control," *Acta Astronaut.*, vol. 54, no. 1, pp. 69–75, Jan. 2004, doi: 10.1016/S0094-5765(03)00194-2.

[9] F.-K. Yeh, "Sliding-mode adaptive attitude controller design for spacecrafts with thrusters," *IET Control Theory Appl.*, vol. 4, no. 7, pp. 1254–1264, Jul. 2010, doi: 10.1049/iet-cta.2009.0026.

[10] Y. Guo, S.-M. Song, and X.-H. Li, "Quaternion-based finite-time control for attitude tracking of the spacecraft without unwinding," *Int. J. Control Autom. Syst.*, vol. 13, no. 6, pp. 1351–1359, Dec. 2015, doi: 10.1007/s12555-014-0318-7.

[11] P. M. Tiwari, S. Janardhanan, and Mashuq un Nabi, "Rigid Spacecraft Attitude Control Using Adaptive Non-singular Fast Terminal Sliding Mode," *J. Control Autom. Electr. Syst.*, vol. 26, no. 2, pp. 115–124, Apr. 2015, doi: 10.1007/s40313-014-0164-0.

[12] M. Jafarboland, N. Sadati, and H. Momeni, "Robust Tracking Control of Attitude Satellite with Using New SMC and EKF for Large Maneuvers," in *2006 IEEE Aerospace Conference*, Big Sky, MT, USA, 2006, pp. 1–10. doi: 10.1109/AERO.2006.1655824.

[13] M. Tarhan and E. Altuğ, "EKF Based Attitude Estimation and Stabilization of a Quadrotor UAV Using Vanishing Points in Catadioptric Images," *J. Intell. Robot. Syst.*, vol. 62, no. 3–4, pp. 587–607, Jun. 2011, doi: 10.1007/s10846-010-9459-y.

[14] H. Kwon, K. Lee, and K. You, "EKF based sliding mode control for a quadrotor attitude stabilization," in *2017 International Conference on Intelligent Informatics and Biomedical Sciences (ICIIBMS)*, Okinawa, Nov. 2017, pp. 101–104. doi: 10.1109/ICIIBMS.2017.8279718.

[15] J. L. Crassidis, F. L. Markley, and Y. Cheng, "Survey of Nonlinear Attitude Estimation Methods," *J. Guid. Control Dyn.*, vol. 30, no. 1, pp. 12–28, Jan. 2007, doi: 10.2514/1.22452.

[16] L'Afflitto, Andrea. A mathematical perspective on flight dynamics and control. Springer International Publishing, 2017.

BIOGRAPHY OF AUTHORS

Adha Imam Cahyadi obtained his bachelor degree in Electrical Engineering from the Department of Electrical Engineering (DEE), Faculty of Engineering, Universitas Gadjah Mada, Indonesia in 2002. Later he got his master in Control Engineering from KMITL in 2005, Thailand and Doctor of Engineering in Robotics and Automation from Tokai University Japan in 2008. Currently he is an Assistant Professor at DEE and serving as the head of Undergraduate Program in Electrical Engineering. His research areas involves application of control theory, robotics and mechanical control systems, telemanipulation systems and Unmanned Aerial Vehicles (UAVs).

Andreas P. Sandiwan obtained his bachelor and master degree in Electrical Engineering at the Department of Electrical and Information Engineering, Faculty of Engineering, Universitas Gadjah Mada, Indonesia. He started his master study in 2019, and finished it in 2021. His research interest involves control systems.

Samiadji Herdjunanto had passed away. He obtained his bachelor degree in Electrical Engineering from Department of Electrical Engineering (DEE), Faculty of Engineering, Universitas Gadjah Mada (UGM). Later he got his master degree from Ohio State University, USA and doctoral degree from Universitas Gadjah Mada. When this manuscript was prepared, Dr Herdjunanto was associate Professor at DEE UGM. His research areas involves adaptive control, signal processing and fault detection.